Advanced Material Characterization via Hybrid Simulation Methods

Elena Vasquez-Gonzalez, Lucas Marquez-Ramirez
Swiss Federal Institute of Technology, Zurich, Switzerland, University of California, Berkeley, USA

Abstract—The nonlinear static and dynamic analysis procedures presented in EN 1998-1 for the structural response of a RC wall-frame building are assessed. The structure is designed according to the guidelines for high ductility (DCH) in 1998-1. The finite element packages Seism Struct and Open Sees are utilized and evaluated. The structural response remains nearly in the elastic range even though the building was designed for high ductility. The overstrength is a result of oversized and heavily reinforced members, with emphasis on the lower storey walls. Nonlinear response history analysis in the software packages give virtually identical results for displacements.
Keywords—Behaviour factor, Dual system, Open SEES, Overstrength, Seism Struct.

I. Introduction

In earthquake prone regions, the forces caused by seismic ground motions are too high to be resisted in the elastic range by structures without excessive member dimensions. Structures are therefore expected to deform past the elastic limit when subjected to a design level earthquake. Several simplified methods have been developed for determination of the seismic response of structures and some of these are incorporated in current design codes. In this paper, a dual system is designed according to such a simplified procedure, i.e. the lateral force method in EN 1998-1 [1], and the resulting seismic performance is evaluated through nonlinear analysis.

Simplified methods for estimating seismic actions given in current design codes take into account ductility and overstrength by reducing forces determined by linear models. In EN 1998-1 [1], the force reduction is incorporated through a behaviour factor q which is chosen based on the structural type (e.g. RC frame or RC dual system) and regularity. The estimation of q has been criticized because ductility in concrete and masonry structures depend on a wide range of factors such as axial loads, reinforcement and geometry [3]. In this paper, the behaviour factor is considered as a product of factors according to the procedure of [4] and [5]. Thus, a ductility factor, μ, and an overstrength factor, Ω, are defined so that [5]

$$q = \mu \times \Omega \quad (1)$$

Here, μ is the ratio between the maximum base shear force that the structure would experience if it behaved linearly to the yield base shear, and Ω is the ratio between the yield base shear and the acting force at the formation of the first plastic hinge [2], [5]. Thus, Ω represents the overstrength of the structure.

The presence of overstrength in buildings is associated with the fact that code-designed structures possess strength beyond the design values. This is due to minimum requirements for member dimensions and reinforcement and conservative determination of material properties and acting loads. The original purpose of the study was to compare the software packages Seism Struct [6] and Open Sees [7]. Throughout the analysis and result processing, the overstrength of the structure proved to be noticeable. Thus, in this paper, the overstrength of a dual system designed for high ductility according to EN 1998-1 is shown to be so comprehensive that the system almost does not experience nonlinear behaviour during a design level earthquake. In the study, both Nonlinear Static Analysis (NSA) and Non-Linear Response History Analysis (NRHA) are applied. The calculations are executed in Seism Struct and Open Sees. The two software packages are used because part of the aim of this study is to compare the somewhat easy-to-use Seism Struct with the more complex Open Sees.

II. Modelling the Prototype Building

A. Geometry and Seismic Loading

The investigated structure is a RC residential building designed for strong earthquakes representing Southern Europe. It withstands lateral forces mainly through shear walls, and vertical loading is mainly carried by frames. I is thus a dual system. The geometry is illustrated in Fig. 1. The structure is designed for ductility class high (DCH) in EN 1998-1, and the design is performed according to EN 1990 [8], EN 1992-1-1 [9] and EN 1998-1. However, the design for gravity loads was performed according to NS-EN 1992-1-1:NA 2008 due to time limitations.

The concrete quality is B25 with 25 mm cover. The strength of the 1st storey wall had to be increased to B45 due to the shear demand. The reinforcement class is B500NC, and the concrete elastic module of stiffness is 25.0 GPa for B25 and 29.8 GPa for B45.

The Peak Ground Acceleration (PGA) is set to 3.5 m/s^2, which

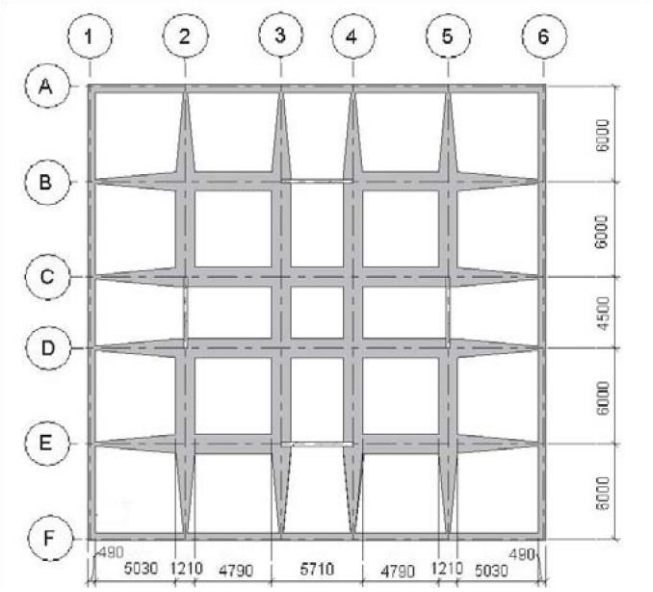

(a) Plan view including the effective beam flanges

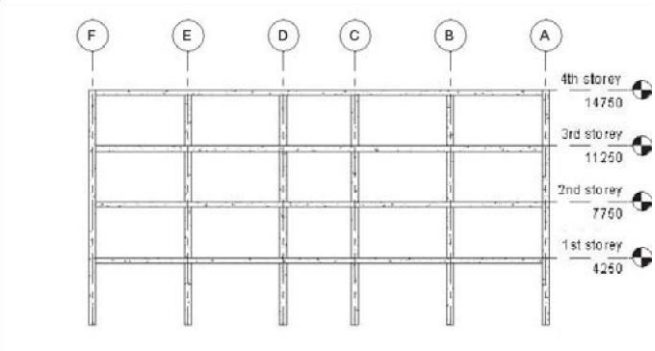

(b) Vertical projection of the structure

Fig. 1 Geometry of the structure

The distributed gravity loads in the seismic situation are $Q_{G,Roof}$ =3 . kN/m and $Q_{G,Storey}$ =4 . kN/m . The system is wall-equivalent with q =3 . . The elastic analysis is performed in Robot [11]. Dead and live loads acting in the seismic design situation are converted to equivalent masses lumped in the stories, m_{roof} =370550 kg, m_{rd} = 383580 kg, m_{nd} =383580 kg and m_{st} =386370 kg. The

$$\delta = 1+1 \quad . \times \frac{X}{L_e}. \tag{2}$$

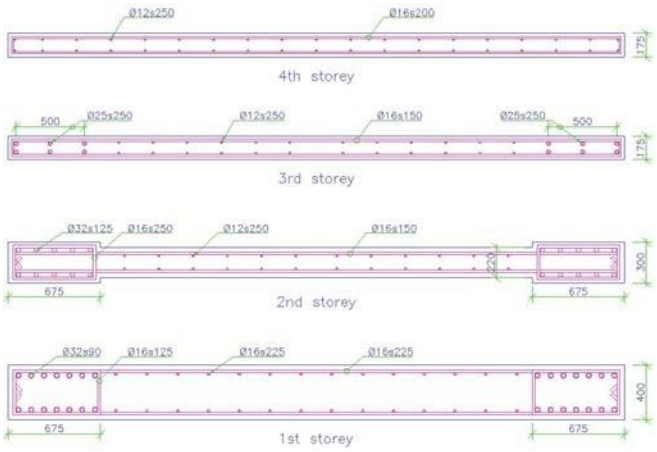

Fig. 2 Wall sections

Here, X is the distance from the mass center to the element in question, measured horizontally, and L_e is the distance between the two elements that resist horizontal forces and are situated farthest from each other.

The beam, column and wall characteristics are presented in Tables I and II, and in Fig. 2.

B. FEM models

The structure is modelled in SeismoStruct and in OpenSees. The first step is to create elastic models which are directly comparable to the already established Robot-model. Next, inelastic materials and elements are introduced. All the nodes are constrained against displacements and rotations out of the plane. The results in this paper are valid for the *entire* structure, not just the half that was modelled.

The material concrete model in OpenSees includes tension softening outside the confined area, whereas the tensile strength in SeismoStruct is abruptly lost when the maximum tensile strain is reached. The reinforcement in OpenSees is modelled using a bilinear steel model that accounts for kinematic hardening. The reinforcement in SeismoStruct has a similar stress-strain relationship up to the fracture/buckling strain =0 . . After this, the strength is lost.

The elastic model consists of beam-column elements. The cross sectional properties are represented by E, I_z and A. In OpenSees, the user must define the above-mentioned parameters manually. This allows the user to include reinforcement when defining the cross section. In SeismoStruct, the user defines a cross section which is assigned to the element type. For reinforced concrete members, the reinforcement is not accounted for when considering stiffness of elastic elements. In this study, it is a goal to create as identical models as possible in the two software packages. Thus, reinforcement is not included in the elastic OpenSees model. Another noteworthy difference between the software packages is that OpenSees consider geometrical nonlinearity on local level for elastic elements whereas SeismoStruct does not. However, P- δ-effects on a

is representative of southern Europe [10]. The elastic and design response spectrum is determined according to EN 1998-1 with ground type C and response spectrum Type 1. stiffness is reduced by 50 % in all columns and beams on account of cracking in the seismic situation. Due to high axial loads, the stiffness in the walls is only reduced by 30 %. The first natural period is 0.51 s. The base shear force F_b is 3718kN. The effective modal masses are 69.7 %, 19.2 %, 0.9 % and 0.5 % for the 1st, 2nd, 3rd and 4th mode, respectively.

The analysis model consists of the frames in axes A, B and C, ref. Fig. 1, connected with rigid links. Thus, the model is in 2D so the effects of accidental torsion are safeguarded by multiplying the acting design forces with a factor

TABLE I
BEAM CHARACTERISTICS

Beam	Top reinf.	Bot. reinf.	l_{cr} (mm)	Stirrups	Stirrups l_{cr}
Border	2φ25	2φ25		φ6c85	φ6c140
Interior beam	3φ32	3φ32+2φ12		φ10c100	φ10c100

TABLE II
COLUMN CHARACTERISTICS

Column	b (mm)	h (mm)	Vert. reinf.	l_{cr} (mm)	Stirrups	Stirrups l_{cr}
Interior			12φ32			16c125 10c120
Border			8φ25			

global level are considered for both elastic and inelastic elements in both programs.

The nonlinear models consists of inelastic force-based beam-column elements that are able to represent bending and axial deformations. They account for inelasticity along the member length and across the sectional area, i.e. they are distributed inelasticity elements. Such elements can be formulated based on two different approaches [12]. The first is the displacement-based formulation (DB), which is the textbook finite element formulation. The element is imposed with a displacement field and the governing equations are solved based on the stiffness. In the assessment of nonlinear problems, such formulations are not ideal. Also, imposing displacement fields when the response is nonlinear may produce spurious results for coarsely meshed models [12]. The other formulation is force-based (FB). Here, instead of displacement fields, force and moment field variations are imposed. The governing equations are solved based on flexibility. The FB-formulation is ”exact” in the sense that it does not restrict the displacement field and thus allows for nonlinear behaviour. The only approximation is the discrete number of Integration Points (IP). The main advantage with the FB-formulation is that only one element is necessary for each structural member due to the fact that the force field is always exact [12], [18].

In both OpenSees and SeismoStruct, the iterative solution procedures are based on the *Newton-Raphson-method* [13]. Due to the nature of structural response caused by seismic loading, prescribed displacement increments are chosen rather than load increments. In OpenSees, other iterative strategies are applied as correction steps. The nonlinear response histories are assessed by the HHT-method. The integration procedure is a modification of Newmark’s method and has the advantage of suppressing high frequency noise more effectively [13]. For the model in question, there is no considerable difference in the dynamic response between the two methods.

III. EIGENVALUE ANALYSIS

In order to investigate the dynamic behaviour of the structure and compare the software packages, several eigenvalue analysis are performed in both programs with varying configuration. The results are illustrated in Fig.

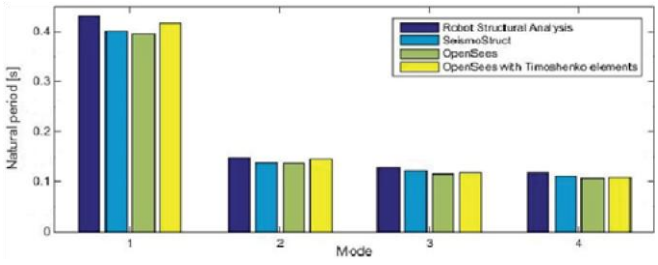

(a) Elastic models

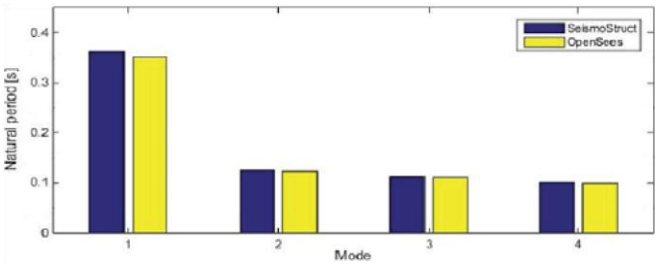

(b) Inelastic models

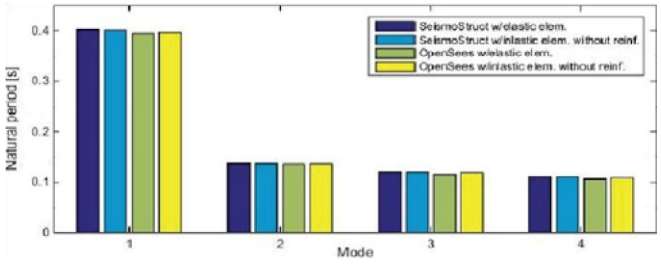

(c) Elastic models versus inelastic models without longitudinal reinforcement

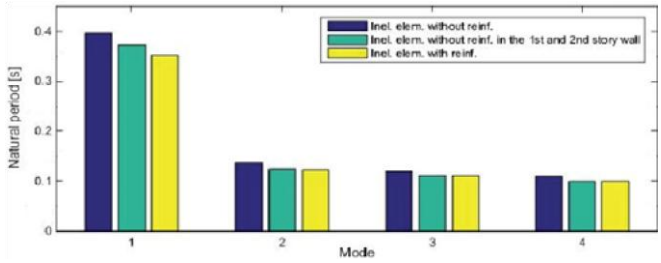

(d) Effects of the 1st and 2nd storey walls (OpenSees)

Fig. 3 Natural periods of the FEM-models

3. The elastic models are compared in Fig. 3a. In this figure, the model in Robot contains no reduction of stiffness, which explains the shorter natural period than what was previously stated. Elastic beam column elements are applied in SeismoStruct and OpenSees, and the figure shows agreement between the results from these programs. The main reason for the slightly softer system in Robot [11] is that the elements in this software package account for shear deformations. This is evident from comparison with the results from OpenSees with and without shear deformations (i.e. elastic beam-column elements vs. Timoshenko beam elements). Accounting for shear increases the 1st natural period by 6 %. SeismoStruct is limited in the sense that it contains no beam-column elements, neither elastic nor inelastic, that account for shear deformations. In OpenSees however, the user can apply the elastic Timoshenko Beam-Column element which directly incorporates shear strains. It is also possible to include shear deformations for inelastic elements through Section Aggregators [14].

Fig. 3b shows compliance between the two packages using inelastic elements. However, comparison with Fig. 3a reveals that the inelastic model is significantly stiffer than the elastic. The reason is that the elastic elements do not account for reinforcement. The inelastic elements, on the other hand, are assigned uniaxial nonlinear materials that accounts for confinement and longitudinal reinforcement. The confined concrete material models are formulated such that the initial stiffness is equal to the non-confined material models. Thus, the difference between the results in Figs. 3a and 3b are due to longitudinal reinforcement. This is documented through the agreement between the results in Fig. 3c where the elastic models are compared to the inelastic models without reinforcement.

The effects of the longitudinal reinforcement in the 1st and 2nd storey walls have been evaluated in OpenSees by establishing a model where the reinforcement in these walls is removed. The results are presented in Fig. 3d and reveal that the first natural period increases significantly as the reinforcement is removed. Fig. 2 shows that the 1st and 2nd storey walls are heavily reinforced at the section ends. Since the cross sectional height is 4.5 m, it is reasonable that the reinforcement in these areas contributes substantially to the bending stiffness. Hand calculation confirms this, the stiffness of the 1st storey wall section is increased by a factor of 1.22 when the reinforcement in the boundary areas is included. Fig. 3d also reveals that the 1st and 2nd storey reinforcement practically does not affect the natural period of the higher modes. This is explained by the fact that the 1st and 2nd storey walls experience high curvature in the first mode, which is illustrated in Fig. 4. The higher modes practically do not curve the 1st and 2nd storey walls. The 2nd, 3rd and 4th mode shapes all show very different deformation of the frames at each side of the wall. This is due to the fact that the frame to the right of the wall is an interior frame and thus has larger mass than the border frame modelled at the left of the wall.

During the comparison of natural periods, differences

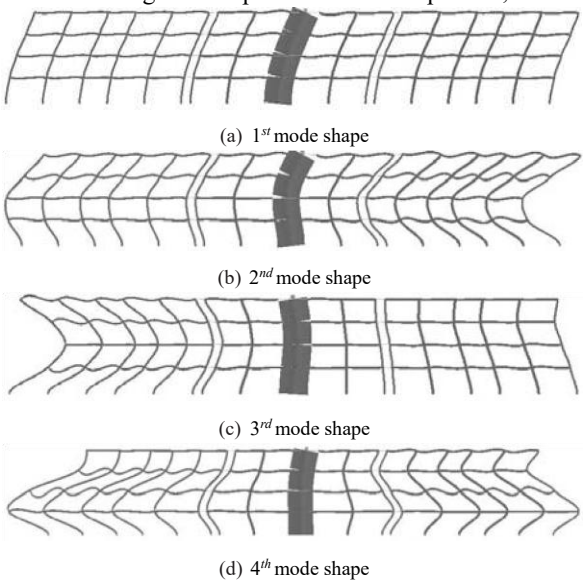

(a) 1st mode shape

(b) 2nd mode shape

(c) 3rd mode shape

(d) 4th mode shape

Fig. 4 First four natural mode shapes of the model according to SeismoStruct

between the elastic and inelastic element types have been revealed. Even though the eigenvalue analysis is a purely elastic analysis, the results suggest that it is not always appropriate to use elastic elements. This applies particularly for SeismoStruct, which provides no possibility of including the stiffness contribution from reinforcement for elastic elements. Also, geometrical nonlinearities on the local level are not considered for elastic elements in SeismoStruct.

In the case of RC structural members, the effects of the longitudinal reinforcement and confined concrete are fully accounted for when applying inelastic elements, without the user having to calculate the sectional properties manually. The effects of the reinforcement vary with the quantity. Members with large cross sectional heights and heavy longitudinal reinforcement, such as the 1st and 2nd storey walls in the investigated structure, are more sensitive to the presence of reinforcement and should

be modelled with inelastic elements even if the user only wishes to carry out the eigenvalue analysis.

IV. Nonlinear Static Analysis

The procedure of NSA is to determine a force-displacement relationship through application of monotonically increasing lateral loads until a horizontal target displacement is reached. The lateral loads represent the inertia forces, and the target displacement represents the maximum displacement expected to occur during a design level earthquake. The mathematical model must directly incorporate the nonlinear stress-strain relationships of all elements expected to deform past the elastic limit. The procedure is not as reliable as NRHA. However, the NSA has the advantage of displaying a clear image of stiffness, strength and ductility [15]. Thus, the analysis method has

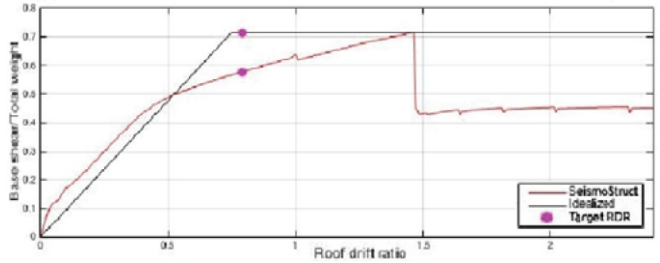

(a) SeismoStruct

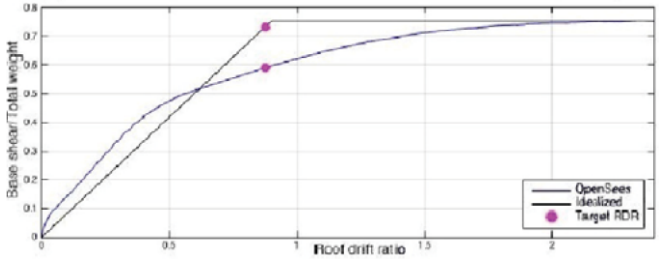

(b) OpenSees

Fig. 5 Pushover curves and resulting idealized curves according to EN 1998-1

advantages to NRHA, and should therefore always accompany NRHA.

EN 1998-1 demand that at least two lateral force distributions are applied during NSA. The first distribution is based on the modal pattern corresponding to the predominant mode, whereas the second is based on the vertical mass distribution regardless of elevation. However, the application of the latter has been shown to underestimate drifts in upper stories and overestimate them in lower stories [16]. Thus, only the mode shape distribution was applied in the analysis. The pushover curves are presented in Fig. 5. The displacement is assessed at the top middle node of the 4th storey wall.

The maximum expected Roof Drift Ratio (RDR) during the design earthquake is determined according to EN 1998-1. The result in SeismoStruct is 0.79% with corresponding base shear/Weight 0.72. The result in OpenSees is RDR 0.87% with corresponding base shear/Weight 0.76. Thus, the difference in target RDR is approximately 10 %, wheras the difference in maximum base shear is only 5 %. The interstorey drifts at target displacement are shown in Fig. 6. The difference between the target RDRs in the two programs is evident in the interstorey drifts, i.e. OpenSees predicts largest drift in all stories. The difference increases from 7% in the 4th storey to 17 % in the 1st. This illustrates that the structure behaves nonlinearly even though it is in the linear range of the idealized pushover curve.

V. Non-Linear Response History Analysis

The NRHA is based on the seven ground motions in Table III, selected from the PEER Ground Motion Database [17]. The selection was based on the following criteria:

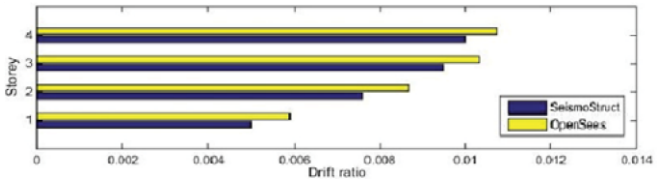

Fig. 6 Interstorey drifts from the nonlinear static analysis

TABLE III
Selected Ground Motions from the PEER Ground Motion Database

RSN	Earthquake	M	r_{up} (m)	V_{s30} (m/s)	PGA (m/s^2)
	San Fernando	6.6			3.04
	Imperial Valley	6.5			4.21
	Superstition Hills-02	6.5			2.16
	Spitak Armenia	6.8			2.65
	Manjil Iran	7.4			2.45
	Joetsu City	6.8			3.43
	Iwate Japan	6.9			2.45

- Solely horizontal far-fault recordings are considered, i.e. $R_{rup} \geq 20km$
- PGA $\geq 2.00 m/s^2$.
- $240 m/s \leq V_{s30} \leq 360 m/s$.
- Moment magnitude larger than 6.5.
- No pulse-like excitation.
- To prevent bias, only one recording from each event was chosen.

The ground motions are scaled to fit the elastic response spectrum in EN 1998-1 at the first natural period of the structure. Such record manipulation seems reasonable due to the fact that the structure in question is heavily dominated by the first mode. The resulting spectra are presented in Fig. 7. The scaling factors are presented in Table IV.

TABLE IV
Ground Motion Scaling Factors

Ground motion	Scaling factor
San Fernando	3.502
Imperial Valley	1.636
Superstition Hills-02	1.837

Spitak Armenia	2.939
Manjil Iran.	1.273
Joetsu City	1.638
Iwate Japan	3.149

The RDR response histories are illustrated in Fig. 8. The roof displacement is assessed at the same node as the target displacement in the nonlinear static analysis. The maximum RDRs and base shear/structural weight are presented in Table V. The maximum interstorey drift ratios are presented in Fig. 9. Fig. 9h shows the average maximum interstorey drift ratios from the seven ground motions.

According to EN 1998-1, the average response parameter of the seven analysis is to be used as the design value. Hence, the expected maximum RDR is 0.800 % according to SeismoStruct and 0.814 % according to OpenSees, and the maximum base shear/weight is 0.739 according to SeismoStruct and 0.870 according to OpenSees.

TABLE V
MAXIMUM RDR AND BASE SHEAR/WEIGHT FROM THE NONLINEAR TIME HISTORY ANALYSIS

Software	Response	S. F.	I. V.	S. H.	S. A.	M. I.	J. C.	I. J.
SeismoStruct	RDR (%)	0.685	0.739	0.536	0.956	0.400	1.11	1.15
	Base shear/Weight	0.909	0.741	0.566	0.846	0.538	0.845	0.828
OpenSees	RDR (%)	0.651	0.746	0.583	0.997	0.427	1.15	1.17
	Base shear/Weight	1.04	0.891	0.681	1.01	0.623	0.970	0.998

Fig. 7 Response spectrum of selected ground motions

VI. DISCUSSION OF THE RESULTS

A. Seism Struct versus Open Sees

The only significant difference between the pushover curves in Fig. 5 is that Seism Struct exhibits a sudden drop around *RDR* = 1.5%. The explanation to the abrupt strength-loss lies in the stress-strain relationship for the reinforcing steel. The response history is thoroughly discussed later, but it should be noted here that the maximum RDRs presented in Table V do not exceed 1.5% for any ground motion and that the individual response history roof displacements presented in Fig. 8 show general agreement between Seism Struct and Open Sees. Seeking to investigate the consequences of the discrepancy in the static analysis, the structure is subjected to the ”Iwate Japan”-ground motion when the scaling factor is increased by 50 %. The response is presented in Fig. 10. There is no compliance between Seism Struct and Open Sees after the RDR reaches approximately 1.5 % at time 25.3 s. The maximum response from Seism Struct exceeds that in Open Sees by a factor of 2.09. Also, the solution in Seism Struct diverges after 37.11 s. It is emphasized that confined material models, geometry, constraints, restraints, element type, applied loads, integrators, algorithms, convergence criteria and damping are consistent throughout the models in SeismoStruct and OpenSees.

The design process revealed that for the elastic range of response, the lateral forces are primarily resisted by the walls. Thus, it is reasonable to suspect that the sudden and significant loss of strength occurs in the walls. The confined concrete material models used in SeismoStruct and OpenSees exhibit smooth and gradual loss of strength. However, the steel model in SeismoStruct exhibits abrupt loss of tensile strength. This limit is defined as the fracture/buckling strain in the material model. In OpenSees, the applied steel model, *Steel01*, does not exhibit such behaviour. The bi-linear relationship is defined soley by the E-modulus, yielding stress and the isotropic hardening factor, i.e. no fracture strain is defined. The fracture limit also explains the difference between SeismoStruct and OpenSees when the structure is subjected to the amplified ”Iwate Japan” ground motion, ref. Fig. 10.

According to EN 1992-1-1 [9], the minimum fracture strain for reinforcement steel in class C is 0.075. Thus, the fracture limit in the steel model applied in SeismoStruct is not conservative, and it complies better with actual material behaviour than the steel model applied in OpenSees [9].

In order to confirm the effects of the fracture limit, a nonlinear static analysis is assessed in SeismoStruct where the fracture strain of the steel model is increased to unity. The pushover-curve is presented in Fig. 11. The responses from SeismoStruct and OpenSees are practically in perfect compliance, expect for the slightly larger maximum base shear force produced by SeismoStruct. The modified model in SeismoStruct is then subjected to the amplified ”Iwate Japan” ground motion and the results are presented in Fig. 12. There are no convergence issues experienced, and SeismoStruct and OpenSees are in nearly complete agreement. The maximum RDR in SeismoStruct exceeds that in OpenSees by a factor of only 1.08.

The individual response history RDRs presented in Fig. 8 show agreement between SeismoStruct and OpenSees. There are some differences though, e.g. the permanent displacement caused by the ”Joetsu City” and ”Manjil Iran” ground motions. In general, OpenSees generates somewhat more conservative results, but the difference is negligible for all practical purposes. OpenSees produces slightly larger interstorey drift ratios, ref. Fig. 9. The average difference between the interstorey drift ratios determined in the two programs is 3%, which is significantly smaller than that found from NSA, ref. Fig. 6. Also, the difference is more even between the stories. Another noteworthy difference between these results and those attained through NSA is that the calculated drifts are smaller in the upper stories. This indicates that the higher mode effects are modest. Contrary to the NRHA results for displacements, there is a clear difference between SeismoStruct and OpenSees in terms of base shear forces. The average difference between the predicted base shear forces is 16 %. A graphical presentation of the maximum displacements and base shear forces is given in Fig. 13. It is observed that base shear forces in SeismoStruct and OpenSees generally correlate less

than displacements, and that for each record, OpenSees generates largest forces. As previously stated, the shear forces predicted through NSA was also largest in OpenSees, but the difference between the programs was modest. In the general finite element method, shear forces are obtained through derivatives which amplify possible errors in the displacement field. Considering force-based elements, i.e. elements where the force field is enforced, the displacements are obtained through integrals [18]. Integrals tend to ”smoothen” out errors, which explains why SeismoStruct and OpenSees agree better in terms of deformations.

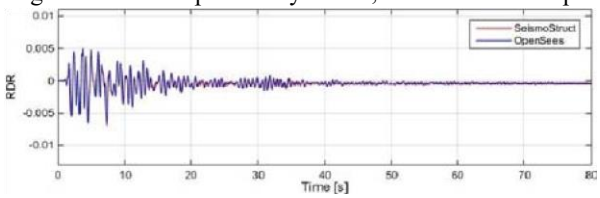

(a) San Fernando

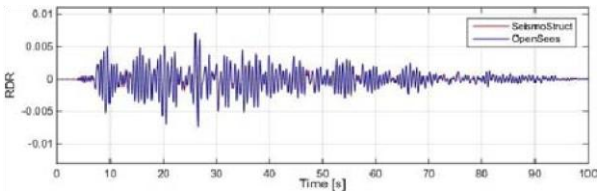

(b) Imperial Valley

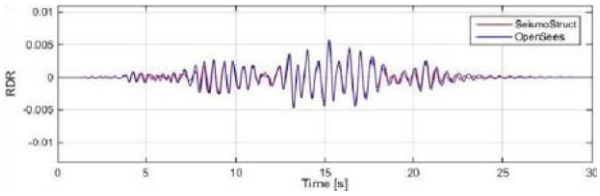

(c) Superstition Hills -02

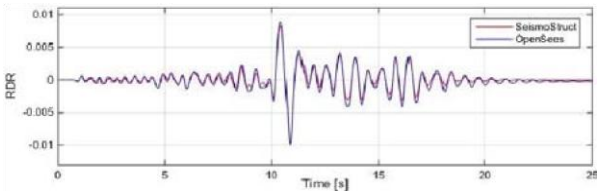

(d) Spitak Armenia

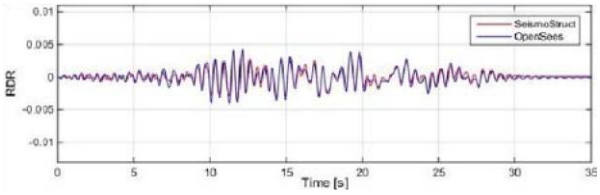

(e) Manjil Iran

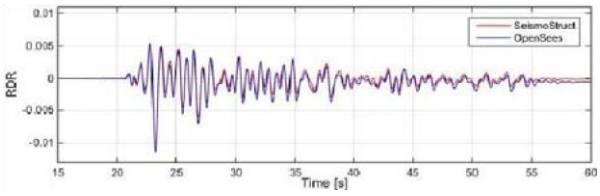

(f) Joetsu City

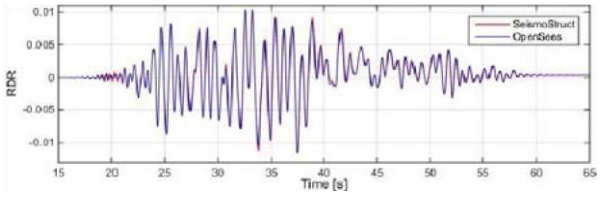

(g) Iwate Japan

Fig. 8 RDR response history

During the ”Joetsu City” and ”Iwate Japan” ground motions, the stress exceeds the yielding limit. The stiffness contribution

B. NSA versus NRHA

Considering the average response from NRHA, the maximum displacements obtained from NSA and NRHA are rather similar. The target RDR error is 10 % in SeismoStruct and 6 % in OpenSees. It has previously been demonstrated, e.g. by Krawinkler and Seneviratna [19], that the nonlinear static analysis is likely to generate reasonable results for structures that primarily vibrate in the first mode, which is the case for the structure in this study. However, there are several uncertainties to be considered. Firstly, the results from the modal analysis in Robot revealed that even though the structure primarily vibrates in the first mode, there was a significant mass contribution from the 2^{nd} mode. Secondly, the ground motions were scaled to fit the first natural period of the cracked system computed in Robot, but Fig. 3a and 3b exposed differences in modal properties between the elastic model in Robot and the inelastic models in SeismoStruct and OpenSees.

Due to these uncertainties, it is interesting to compare *individual* response history results with the results from NSA as presented together in Fig. 13. It should be noted that the maximum base shear force and displacement do not necessarily occur simultaneously. The figure reveals that even though the average response from NRHA is almost in perfect match with NSA considering maximum RDR, there are still large discrepancies between the individual responses.

Fig. 7 shows that out of the seven ground motions, San Fernando induces the highest spectral accelerations for $0 \leq T \leq 0.4$. The first four natural periods of the structure are within that range, ref. Fig. 3, but the largest displacements are caused by the Iwate Japan and Joetsu City ground motions which dominate the scaled response spectrum for periods around 0.65-0.70 s, ref. Figs. 7 and 13. This is due to global softening, mainly related to cracking. The natural periods of the building presented in Fig. 3 are based on the non-cracked system. As previously mentioned, the response spectrum was fitted to match the first natural period of the structure calculated in Robot with 50 % stiffness reduction for beams and columns and 30 % for walls. Even though calculated in Robot [11], which generally gave softer systems, the reduction of stiffness was perhaps not sufficient. Reducing the walls stiffness to 50 % of the original stiffness in Robot increases the 1st natural period to 0.59, which is still lower than the period region dominated by the ”Iwate Japan” and Joetsu City” ground motions.

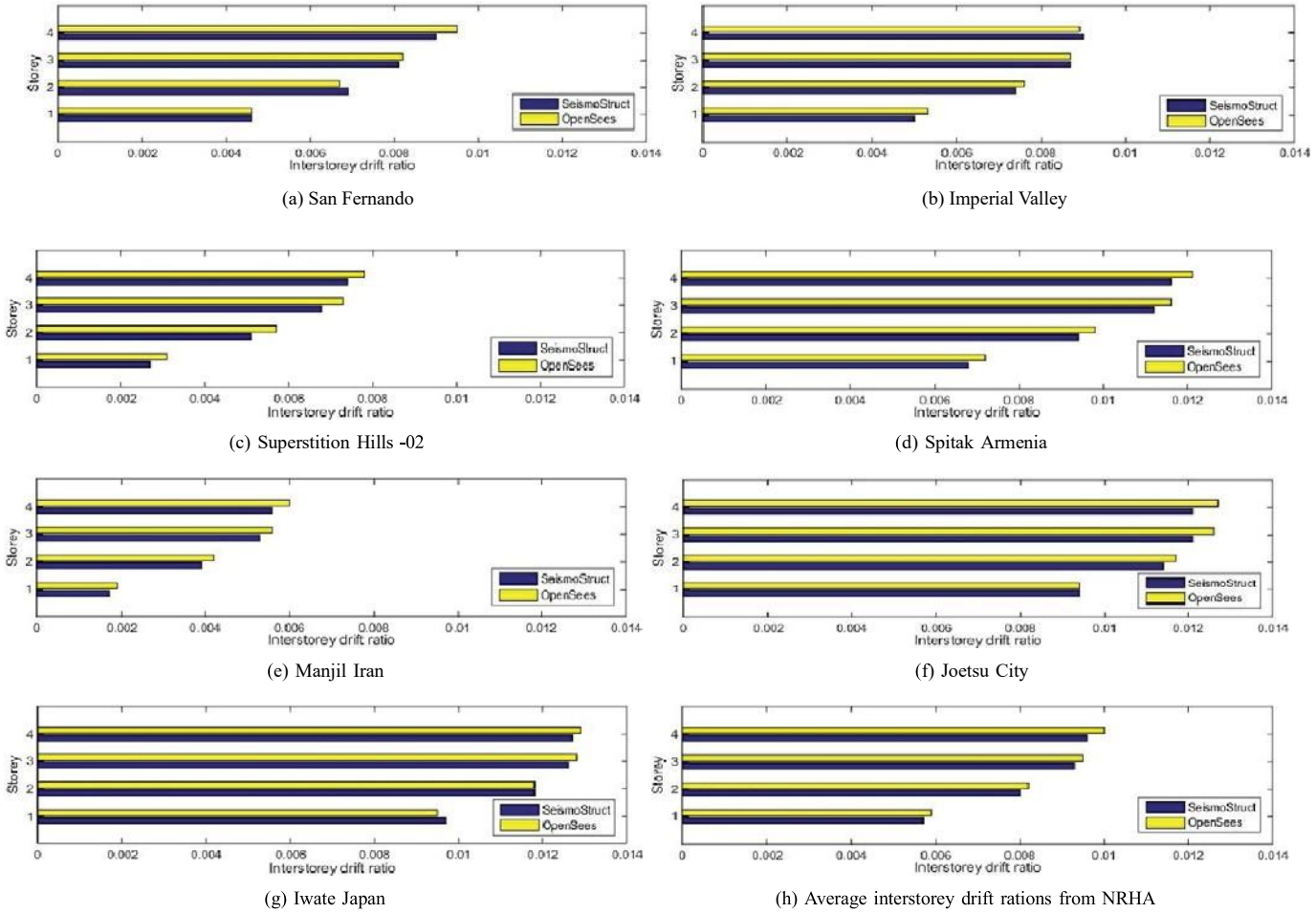

(a) San Fernando (b) Imperial Valley

(c) Superstition Hills -02 (d) Spitak Armenia

(e) Manjil Iran (f) Joetsu City

(g) Iwate Japan (h) Average interstorey drift rations from NRHA

Fig. 9 Maximum interstorey drift ratios from the nonlinear time history analyses

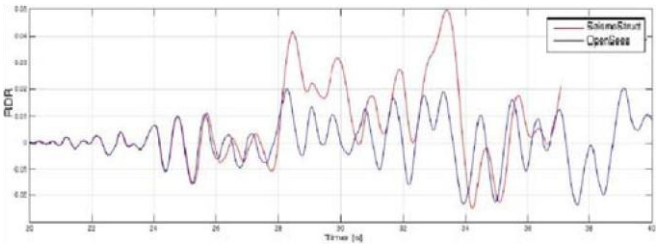

Fig. 10 Displacement response of the control node for ”Iwate Japan”-ground motion increased by 50 %

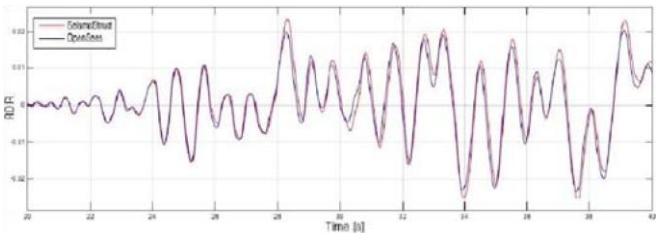

Fig. 12 Displacement response of the control node for ”Iwate Japan” ground motion increased by 50 % when the fracture strain of reinforcement steel in SeismoStruct is set equal to unity

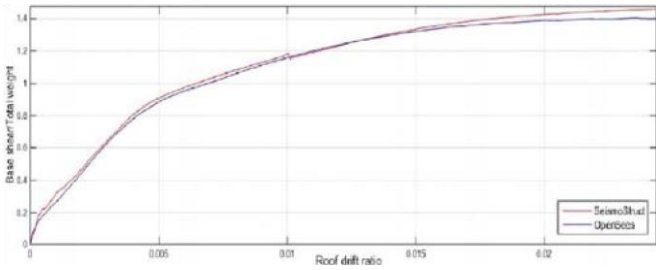

from the reinforcing bars is negligible once yielding is reached, but retained when the stress is reduced later in the cycle. As illustrated in Fig. 3, the modal properties of the structure are sensitive to the presence of reinforcement due to the heavily reinforced shear walls. However, the magnitude of the modal alterations were not in the same scale as the global softening that apparently occurs during the excitation from the response history records. This indicates that the effects of cracking are of much greater significance than yielding of reinforcement when considering global softening.

Fig. 11 Normalized base shear-control displacement relationship. The fracture strain of reinforcement steel in SeismoStruct is set equal to unity

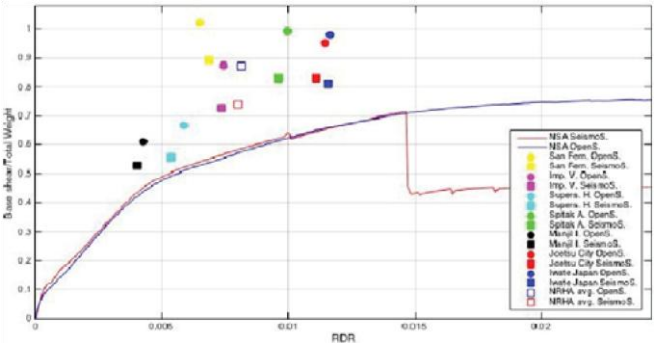

Fig. 13 Pushover curve and maximum RDR and base shear from NRHA

NSA at target displacement. Observe that the difference is larger in OpenSees than in SeismoStruct, ref. Fig. 13. This is

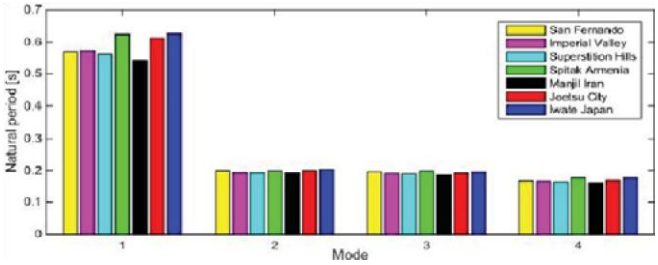

Fig. 14 Natural periods of the cracked system. Eigenvalue analysis has been performed after the structure has been exposed to the individual ground motion

The results from NRHA suggest that the period is increased by a factor of approximately two during the earthquake. Thus, the general expression for the natural period,

$$T = 2 \times \pi \times \sqrt{\frac{m}{k}} \tag{3}$$

implies that the global stiffness has been reduced by a factor of 0.25. Similar results are obtained from the nonlinear static analysis: the global stiffness reduction factor attained during the course of loading, i.e. the difference between the initial and idealized curve slopes in Fig. 5b, is 0.27.

The level of cracking varies with the ground motion loading, which implies that the period elongation is not consistent during different earthquakes. Individual eigenvalue analysis has therefore been performed after exposure to each ground motion record, and the results are presented in Fig. 14. The analyses are performed solely in OpenSees. To the authors knowledge, SeismoStruct offers no possibility of evaluating the eigenvalue problem post a static or dynamic analysis. The prolonged 1^{st} natural periods caused by ”Iwate Japan” and ”Joetsu City” are equal to 0.63 s, which is equivalent of a first natural period prolongation factor of 1.8 for the inelastic system, i.e. the natural periods depicted in Fig. 3c. This corresponds to a global stiffness reduction factor equal to 0.30. ”Manjil Iran” causes the lowest period elongation. The first natural period is 0.54 s, corresponding to a global stiffness factor reduction of 0.42. The average stiffness reduction factor during NRHA is 0.36, which is markedly lower than the 0.50 recommended in EN 1998-1. This is typical for reinforced concrete structures since the value 0.50 is a compromise between predicting realistic displacements and prescriping conservative inertia forces [20].

Comparison of Figs. 3c and 14 shows that the effects of cracking have largest impact on the first mode. Altogether, the maximum RDRs acquired from the nonlinear response history analysis become more intuitive compared with the scaled response spectra when the structure with prolonged natural periods is considered.

The maximum base shear forces from the response histories are considerably higher than the base shear force obtained in

in compliance with a study presented in FEMA 440 Appendix F [21]. The discrepancy is largest for the San Fernando ground motion which, as prevously noted, has the largest high frequency content, ref. Fig. 7.

C. Requirements in EN 1998-1

The structure was designed for high ductility in accordance with the guidelines given in EN 1998-1. The modification factor q was determined equal to 3.51. In accordance with the definition of the behaviour factor in equation (1), and with reference to the pushover curves presented in Fig. 5, the force reduction factor μ is equal to $1.06 \approx 1$ for

SeismoStruct and unity for OpenSees. This implies that despite the expectation of and design for high ductility, the structural response of the idealized system remained in the elastic range. The overstrength factor, Ω equals 1.6 for SeismoStruct and 1.8 for OpenSees. The behaviour factor q is thus equal to 1.7 according to SeismoStruct and 1.8 in OpenSees. The code-based q exceeds the assessed q by a factor of 2.1 for SeismoStruct and 2.0 for OpenSees.

There are three main reasons for this divergence. One is that the idealized system as defined in EN 1998-1 experiences constant stress after yielding, ref. Fig. 5. The result is a larger elastic region than if strain hardening was allowed for. This is evident from the discussion of Fig. 6. The second reason for the overstrength is the way accidental torsion was considered in the design. It is thus recommended that buildings are modelled in 3D, which leads to replacement of the factor 1.2 with 0.6 in equation (2). The third reason is the shear capacity requirements for walls in DCH which are given in EN 1998-1, clause 5.5.3.4.2 and 5.5.3.4.3. The former section evaluates compression failure due to shear. Clause 5.5.3.4.3 evaluates tension failure due to shear, and states that if a wall height factor α_s is larger than 2.0, the wall is considered slender and expected to fail in moment. Then the shear capacity is determined in accordance with EN 1992-1-1 [9]. If α_s is less than or equal to 2.0, the wall is considered stump and expected to fail in shear. The shear capacity is therefore determined through a comprehensive set of

guidelines that increase the dimensions, thus decreasing the 1st natural period which again increase the base shear. For the 1st storey wall, the combination of acting moment, shear force and wall length resulted in α_s less than 2.0, thus implying a stump wall. For

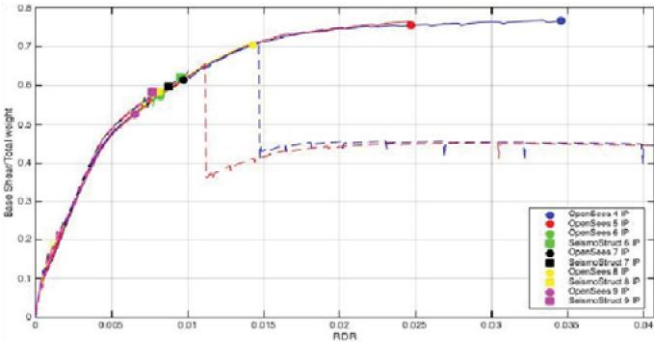

Fig. 15 Nonlinear analysis with varying number of integration points. Filled circles and squares indicate divergence

the same wall, the shear forces were increased according to clause 5.5.2.4.1 due to redistribution of forces and possible dynamic effects related to slender walls. This is the main reason for the large thickness of the 1st storey wall. These three factors resulted in a structural system that did not exhibit highly ductile behaviour when exposed to ground motions that matched the elastic response spectrum provided by the code even though it was designed in DCH.

The underestimation of the stiffness reduction of the walls, i.e. reduction by 30 % instead of the prescribed 50 % has negligible influence on the base shear capacity and overstrength because the first natural period of the structure falls in the constant part of the design spectrum.

D. Effect of Integration Points

Prior to achieving the desired pushover curves and response histories, convergence issues were experienced in both SeismoStruct and OpenSees. Originally, force-based elements with seven integration points were applied. Even though multiple solution strategies were tried by altering integrators, algorithms, time-steps etc., the solution always diverged before the target displacement was reached or response history analysis completed. It is therefore interesting to investigate the consequences of number of IPs in both SeismoStruct and OpenSees in terms of convergence. The analyses performed in the study were based on force-based beam-column elements with four integration points.

The effects of increasing the number of integration points is evaluated through the NSA. The building is ”pushed” to a RDR of 4 % and the pushover curve is presented in Fig. 15. The filled circles and squares indicate where divergence occurs. Evidently, the solution in SeismoStruct converges for 4 and 5 integration points, but diverges for every other configuration. It is observed that the displacement at which the solution diverges decreases with increasing number of integration points. The same trend is however not observed in OpenSees, where convergence issues occur somewhat randomly considering the number of IPs.

The only significant difference between the converging curves is that the drop in SeismoStruct occurs at different displacement steps when applying 4 and 5 integration points.

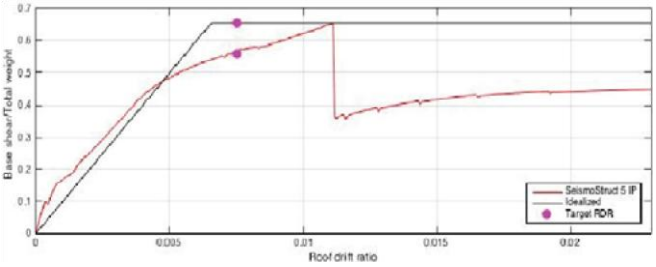

Fig. 16 NSA in SeismoStruct with 5 integration points

Comparison of Fig. 15 and Table V reveals that this would affect the NRHA for 5 of the 7 ground motions. Unfortunately, it is not possible to complete NRHA with 5 IPs due to convergence problems, but the idealized pushover curve based on the analysis with 5 IPs is presented in Fig. 16. The target displacement corresponds to RDR = 0.770 %, and the resulting base shear/weight is 0.56. The target roof drift ratio is thus almost identical to that with 4 IP, but the corresponding base shear is reduced. The level of ductile behaviour according to (1) is larger with 5 IPs than with 4, but the difference is negligible.

Thorough evaluation of force-based inelastic elements is beyond the scope of this paper and will not be further discussed. The reader is referred to the literature [12], [18].

VII. Conclusion

A. Dynamic versus Static Procedures

The results revealed that NRHA prescribed larger base shear forces than NSA. The largest discrepancies were experienced for ground motions with significant high frequency content. The static analysis, within its range of validity, enabled for confirmation of the NRHA results.

B. SeismoStruct versus OpenSees

SeismoStruct has the clear advantage of a graphical interface that allows for easy and time-efficient modelling of structures. In addition, the user is able to evaluate response parameters graphically without the use of external applications, which is of great convenience in the early stages of model establishment. Compared to OpenSees, SeismoStruct is limited in terms of element assortment, algorithms, integrators and output selection. It also lacks elements that take into account shear deformations. OpenSees has the advantage of flexibility and is thus generally more robust, both in terms of equation solving and structural configuration. In addition, OpenSees allows for solving the eigenvalue problem post analysis and thus assessing the modal properties for RC-systems in the cracked state. The response quantities from the two software packages generally matched

except for the following: . The steel model applied in OpenSees did not include steel failure, and the pushover curve thus did not drop when the 1st storey wall reinforcement should have lost strength. Thus, this steel model is not recommended in shear walls.

- OpenSees generated higher target RDR than SeismoStruct in NSA.
- OpenSees generated higher base shear forces than SeismoStruct in NRHA, but similar base shear in NSA.

C. EN 1998-1

Even though the structure was designed for high ductility, the structural response remained nearly in the elastic range. The elastic behaviour was a result of oversized and heavily reinforced members, with emphasis on the lower storey walls. The reduction of global stiffness during NRHA was greater than the recommendation in EN 1998-1. The stiffness reduction factor varied from 0.31 to 0.42, depending on the ground motion, whereas EN 1998-1 provide a general factor of 0.5.

Accidental torsion was considered in a way that leads to overstrength. Due to the fact that the results show excessive overstrength, it is recommended that buildings are modelled in 3D so that the demands due to accidental torsion are reduced.

D. Number of IPs

The number of IPs proved to be significant for the calculated base shear capacity. In SeismoStruct, application of 5 IPs instead of 4 did not affect the target displacement, but the NRHA with 5 IPs did not converge. Based on the effect on the number of IPs on the placement of the drop in the pushover analysis, the effect on number of IPs on shear walls should be the subject of future research.

REFERENCES

[1] De Normalisation, Comite Europ´ een,´ *Eurocode 8: Design of structures for earthquake resistance: Part 1: General rules, seismic actions and rules for buildings*, European Committee for Standardization, 2004.
[2] Cemalovic, Miran, Earthquake analysis og structures using non-linear models, Masters thesis, Norwegian University of Science and Technology (NTNU), Department of Structural Engineering, 2015
[3] Priestley, M.J.N. and Calvi, G.M. and Kowalsky, M.J., Direct displacement-based seismic design of structures, 2007 NZSEE Conference, 2007.
[4] Kappos, A.J., Evaluation of behaviour factors on the basis of ductility and overstrength studies, Engineerning Structures, Volume 21, 1999.
[5] Asgarian, B. and Shokrgozar, H, Brbf response modification factor, Journal of constructional steel research, Volume 65, no. 2, pp. 290-298, 2009.
[6] SeismoStruct, SeismoStruct is a FEM-program developed for the analytical assessment of structures subjected to earthquake strong motion, Seismosoft Ltd, Version 7.0.2, 2015.
[7] OpenSees, The Open System for Earthquake Engineering Simulation (OpenSees) is a software framework for simulating the seismic response of structural and geotechnical systems, Pacific Earthquake Engineering Research Center, Version 2.4.5, 2013.
[8] Comite Europ´ een de Normalisation, Eurocode 0: Basis of Structural´ Design, European Committee for Standardization, 2008
[9] Comite Europ´ een de Normalisation, Eurocode 2: Design of Concrete´ Structures: Part 1: General Rules and Rules for Buildings, European Committee for Standardization, 2010
[10] Robot, Robot Structural Analysis Professional is an BIM-integrated FEM-software developed for the assessment of structural analysis and memeber design, Autodesk, Inc., Version 2.4.5, 2013.
[11] Calabrese, Armando and Almeida, Joao Pacheco and Pinho, Rui,˜ Numerical issues in distributed inelasticity modeling of RC frame elements for seismic analysis, Journal of Earthquake Engineering, Volume 14, 2010, Taylor & Francis.
[12] Cook, Robert D. and Malkus, David S. and Plesha Michael E. and Witt, Robert J., Concepts and applications of finite element analysis, John Wiley and Sons, INC., 4th edition, 2002.
[13] Fajfar, Peter and Dolsek,˜ Matjaz,˜ Pushover-based analysis in performance-based seismic engineering - A view from Europe, Springer Science+Business Media Dordrecht, 2014.
[14] Goel, Rakesh K. and Chopra, Anil K., Evaluation of modal and FEMA pushover analyses: SAC buildings, Earthquake Spectra, Vol. 20, Pages 225-254, 2004.
[15] Gharakhanloo, Armin, Distributed and Concentrated Inelasticity BeamColumn Elements used in Earthquake Engineering, 2014.
[16] Krawinkler, Helmut and Seneviratna, G.D.P.K., Pros and cons of a pushover analysis of seismic performance evaluation, Engineering structures, Vol. 20, Page 452-464, 1998, Elsevier.
[17] Elghazouli, Ahmed, ed., Seismic design of buildings to Eurocode 8, CRC Press 2009.
[18] Applied Technology Council, FEMA-440 - Improvement of non-linear static seismic analysis procedures, Redwood City, 2005.